論文 / 著書情報
Article / Book Information

論題	
Title	A New Flexure Revolute Joint with Leaf springs and Its Application to Large Workspace Parallel Robot
著者	米本 慶治, 武田 行生, Tou Sei, 樋口 勝
Author	Keiji YONEMOTO, Yukio TAKEDA, Zheng TONG, Masaru HIGUCHI
掲載誌/書名	, Vol. 6, No. 1, pp. 76-87
Journal/Book name	Journal of Advanced Mechanical Design, Systems, and Manufacturing, Vol. 6, No. 1, pp. 76-87
発行日 / Issue date	2012, 1
URL	http://search.ieice.org/
権利情報 / Copyright	本著作物の著作権は日本機械学会に帰属します。
Note	このファイルは著者（最終）版です。 This file is author (final) version.

Journal of Template

Vol. 00, No. 0, 0000

A New Flexure Revolute Joint with Leaf springs and Its Application to Large Workspace Parallel Robot*

Keiji YONEMOTO**, Yukio TAKEDA**, Zheng TONG**,
and Masaru HIGUCHI***

** Department of Mechanical Sciences and Engineering, Tokyo Institute of Technology
2-12-1, Ookayama, Meguro-ku, Tokyo 152-8552, Japan

*** Department of Innovative Systems Engineering, Nippon Institute of Technology
4-1, Gakuendai, Miyashiro-machi, Minamisaitama-gun, Saitama 345-8501, Japan

Abstract

This paper presents a flexure revolute joint with a large range of motion which can be used as a joint in a parallel robot with a large workspace. We proposed a new structure of flexure revolute joint. The joint consists of leaf springs which are symmetrically arranged between two frames. The shape of the frame is like a spiral stairs. Arrangement of leaf springs was proposed taking into consideration the axis drift and stiffness characteristics of the joint while achieving a large range of motion. Characteristics of the proposed joint were investigated by Finite Element Analysis (FEA) and experiments. A planar parallel robot with two degrees of freedom using the proposed joints was designed and fabricated. Its workspace, position repeatability and stiffness were experimentally investigated.

Key words: Robotics, Parallel Robot, Machine Element, Flexure Joint, Range of Motion, Accuracy, Stiffness

1. Introduction

With the improvement in IC and MEMS manufacturing technology, high precision and large workspace robots which can operate in a vacuum are strongly required. As for robots used for surgery and food production, pollution free operation and easiness of washing are required. Joints used in such robots should not have friction because it causes heat and dust. Lubrication of joints also becomes a source of pollution to the operation space and objects. Actuators had better to be placed in an isolated space from the operation space to let them operate in a better environment to avoid sealing and heat problems.

Parallel robot with flexure joints is one of the appropriate candidates for such applications. Parallel robot is a type of robots with several kinematic chains supporting the output link. They can precisely achieve tasks compared to serial ones because errors of kinematic chains are averaged. Actuators of parallel robots can be easily isolated from the operation space by placing them on the stationary base.

Flexure joint provides a relative motion between links using elastic deformation of the components. It has no backlash and diminished friction because they don't use rolling and sliding contacts. This leads to higher resolution of the motion compared with joints using rigid contacts such as ball bearings and sliding guides. Since flexure joint does not need lubrication [1], it does not generate dust and it can be easily washed. On the other hand, flexure joint has some drawbacks. Its range of motion is limited and is not so large in general. It has resistant stiffness, and its off-axis stiffness is not as high as that of joint using rigid contacts. Its motion axis has non-zero drift according to its motion [2].

In literature, various types of flexure joints with a large range of motion have been

*Received XX Xxx, 200X (No. XX-XXXX)
[DOI: 00.0000/ABCDE.2006.000000]

proposed. Zhao et al.[3] proposed a compound generalized cross-spring pivot composed of a pair of crossed springs with optimized arrangement of the springs to reduce off-axis motion. Its range of motion is up to 30 deg. Trease et al.[2] compared several types of flexure joints and introduced three criteria for design of flexure joints, which are range of motion, amount of axis drift and ratio of off-axis stiffness to the axial stiffness. They proposed a new type of flexure revolute joint which utilizes torsional deformation of thin plates. It has a range of motion of 34 deg, high stiffness ratio and no axis drift with its rotation. Arata et al. [4] proposed a two degree-of-freedom bending manipulator using elastic deformation of leaf springs. Although this joint achieved a bending angle up to 60 deg, it includes sliding contact elements and has insufficient capacity to support a large external load. Flexure joints with larger range of motion are still demanded which can be applied to a large workspace robot.

In the present paper, we proposed a new flexure revolute joint with leaf springs. To develop a flexure revolute joint with large range of motion, improved axis drift and stiffness ratio compared with conventional ones, the proposed joint features use of multiple leaf springs, symmetrical arrangement of leaf springs and prevention of compressive and torsion loads in leaf springs. The composition of the joint is clarified and characteristics of the joint are theoretically and experimentally investigated. We designed and fabricated a planar parallel robot with the proposed flexure revolute joints, and investigated its characteristics.

2. Proposition of Flexure Revolute Joint

2.1 Design Concept

Most of flexure joints can be classified into two types: notch type and leaf spring type. Notch type joints are fabricated by making a semicircle or hemisphere shaped notch on a beam. This type is used in high precision robots with a small workspace such as microscope focusing mechanism, in which precise motion within a very small range of motion is required to the joint [5]. Leaf spring type joint utilizes elastic deformation of leaf springs. Motion range of this type is large. However, since a simple leaf spring has low stiffness in bending and torsional deformations, it doesn't work as a joint with a single degree of freedom. The buckling of leaf springs occurs when large compressive force is applied. Predicting the deformed shape and stiffness of leaf springs is not easy. Some prediction methods have been presented [6][7], but it's still difficult to clarify the deformed shape and the stiffness when off-axis force is applied to the leaf spring.

In the present paper, we propose a new structure of flexure revolute joint using leaf springs. Our basic concept to cope with the problems mentioned above is using multiple leaf springs and arranging them symmetrically in a space. Figure 1 shows the basic configuration of the proposed joint. It is composed of two frames and several leaf springs. The decoupled parts of the joint are shown in Fig.2. The composition shown in Fig. 2 is the same as that of the experimental joint that is discussed in chapters 4 and 5. The shape of the frame is like a "*spiral stairs*" and two frames are connected by the leaf springs. At each step of "stairs" of a frame, one end of a leaf spring is connected with a washer and bolts. Each of the two links of a robot is rigidly connected to one of the frame of the joint. The two links connected by the joint can relatively rotate around the rotation axis shown in Fig. 1. As shown in Fig. 1, directions of relative motion of the frames and applied load, which are denoted as "rotation", "translation", and "torsion", are defined taking the rotation axis as the basis. The characteristics of the joint are dependent on the arrangement of leaf springs. Arrangement of the leaf springs will be discussed in the following section.

2.2 Arrangement of Leaf Springs

We considered the following four conditions to determine the effective arrangement of leaf springs to realize the concept mentioned in the previous section.

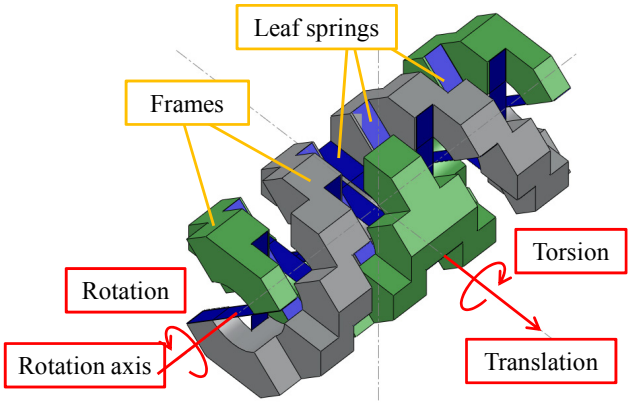

Fig. 1 Configuration of the proposed flexure joint

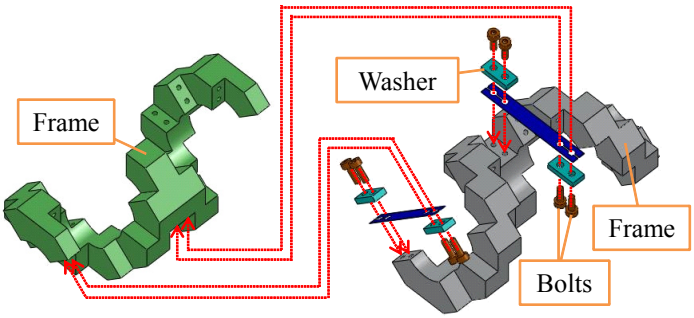

Fig. 2 Decoupled parts of the joint

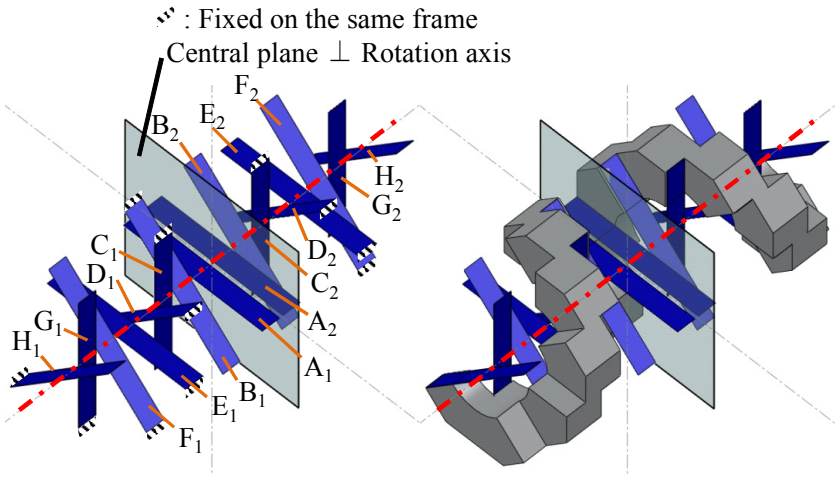

(a) Leaf springs (b) Frame

Fig. 3 Structure of the proposed flexure joint

(1) The leaf springs are symmetrically arranged to the rotation axis to reduce the variation of stiffness of the joint.
(2) Only the bending of the springs is utilized to generate the motion of the joint by constraining torsional motion of the springs.
(3) The compressive loads on leaf springs are avoided to prevent their buckling.
(4) The whole leaf springs are symmetrically arranged to the central plane, which is perpendicular to the rotation axis (see Fig. 3(a)), to reduce the axis drift caused by the unbalance of the reaction forces exerted between the frames by the leaf springs.

The arrangement considering the above conditions is shown in Fig. 3(a). This figure

shows the neutral configuration of the joint for the case where sixteen leaf springs (A_1~H_1, A_2~H_2) are arranged at an equal distance and an equal offset angle of 45deg around the joint axis. Here, the neutral configuration of joint is defined as the configuration where all the leaf springs are not deformed at all, and are straight. This arrangement of the leaf springs was determined as the following "strategies" to cope with the conditions mentioned above. Here, the strategy's number basically corresponds to the condition's number.

(1) Leaf springs with subscript "1" are arranged at an equally spaced angle around the joint axis.

(2) Two of the springs with subscript "1" compose a pair so that they are perpendicular to each other (e.g. A_1 and C_1).

(3) Two of the springs with subscript "1" compose a pair so that one spring of the pair is located in the position obtained by rotating the other spring of the pair around the rotation axis by π (e.g. A_1 and E_1).

(4) The arrangement of the leaf springs with subscript "2" is the same as that of springs with subscript "1" and they would be placed at the mirrored position of those of "1" to the central plane.

The arrangement based on the strategy (1) corresponds to the condition (1) to reduce the directional variation of the stiffness of the joint. The arrangement based on the strategy (2) corresponds to the condition (2) to prevent torsional deformation of leaf springs (e.g. leaf spring A_1 constrains the motion which leads to torsional deformation of C_1 in Fig. 3(a), and vice versa). The arrangement based on the strategy (3) corresponds to the condition (3) to prevent buckling of leaf springs because forces exerted between the frames are supported by tension forces of leaf springs and no compression force is exerted on the springs. The arrangement based on the strategy (4) corresponds to the condition (4) to prevent axis drift according to the rotational motion of the joint by good balance of reaction forces by the leaf springs. Other combinations of leaf springs are also acceptable if the same strategy is applied (e.g. twenty four leaf springs with an offset angle of 30 deg).

2.3 Configuration of Joint Frame

To realize the arrangement of leaf springs proposed in the previous section while avoiding the interference between frames, we designed the shape of the frame. As mentioned above, its shape is like a spiral stairs as shown in Fig. 3 (b). Interference of frames was checked within the range of motion using a 3D-CAD software.

3. Numerical Analysis of Flexure Revolute Joint

3.1 FE Model

We investigated the characteristics of the proposed joint by the finite element analysis (FEA) to validate the concept and structure of the joint and to determine appropriate dimensions of leaf springs. We assumed that the frames of the joint are rigid and the leaf springs are made of hardened steel. In the following part of this paper, joints with sixteen leaf springs are considered. Mechanical properties of the leaf springs are shown in Table 1. Fabrication errors were not considered. In the finite element (FE) model, each leaf spring consists of 1,280 hexahedron elements and is assumed as nonlinear element. The model used in FEA and an example of the analysis results are shown in Fig. 4. Abaqus/standard was used to solve FEA under nonlinear conditions.

3.2 Analysis Result

Relationships between displacements and loads are shown in Fig. 5. Directions of motion and load are indicated in Fig. 1. It is known from the figure that the joint has constant stiffness about each direction. The stiffness in each direction was calculated from the results by the least square approximation. The range of motion was defined as the range

Table 1 Properties of the leaf springs

Length	18mm
Width	5mm
Thickness	0.15mm, 0.1mm
Young's modulus	210GPa
Poison's ratio	0.3
Yield stress	1GPa

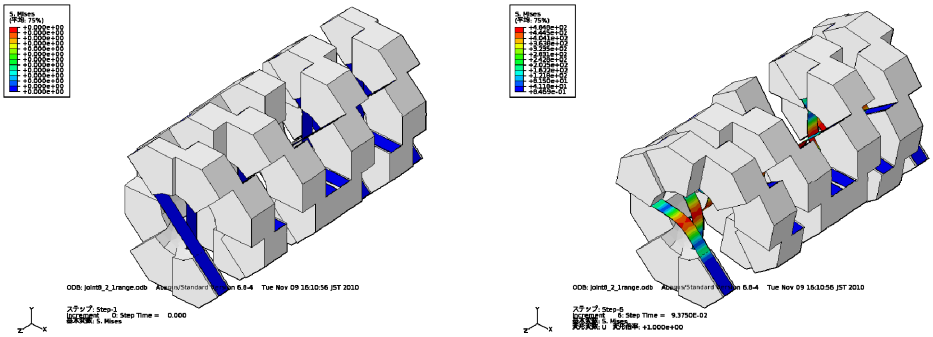

(a) Neutral configuration (b) Deformed shape

Fig. 4 FE model

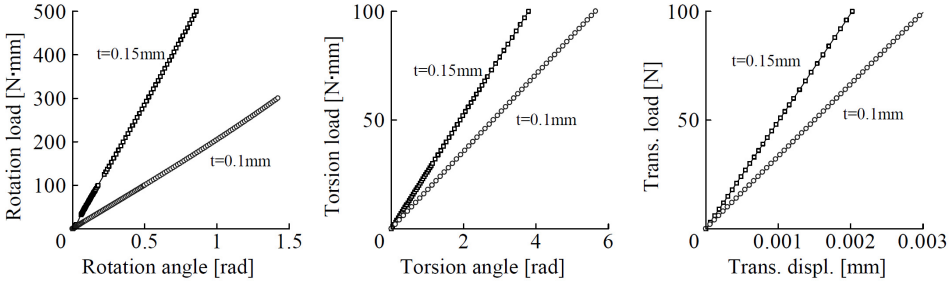

(a) Rotation (b) Torsion (c) Translation

Fig. 5 Displacement-load relationship of the proposed joints obtained by FEA

Table 2 Characteristics of the proposed joint obtained by FEA

Leaf spring thickness [mm]		0.15	0.1
Range of motion [deg]		90	140
Stiffness	Rotation [N mm/rad]	5.8×10^2	2.1×10^2
	Torsion [N mm/rad] (Ratio [-])	2.6×10^7 (4.5×10^4)	1.8×10^7 (8.5×10^4)
	Translation [N/mm] (Ratio [rad/mm^2])	4.9×10^4 (85)	3.3×10^4 (1.6×10^2)

where the maximum stress of the leaf springs is within the yield stress.

The characteristics obtained from FEA results are summarized in Table 2. It is known from the table that the proposed joint can achieve a large range of motion and a large stiffness ratio. Here, stiffness ratio is defined as the ratio of the off-axis (torsion and translation) stiffness to that around the joint axis (rotation). Axis drift obtained by FEA was negligibly small. These results validate the structure of the proposed joint. It is also found that the thinner leaf spring (0.1 mm thickness) leads to better characteristics of the joint in terms of range of motion and stiffness ratio.

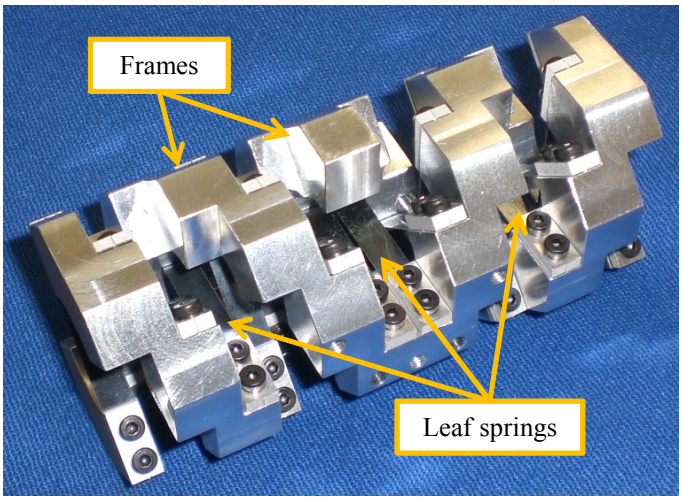

Fig. 6 Overview of experimental joint

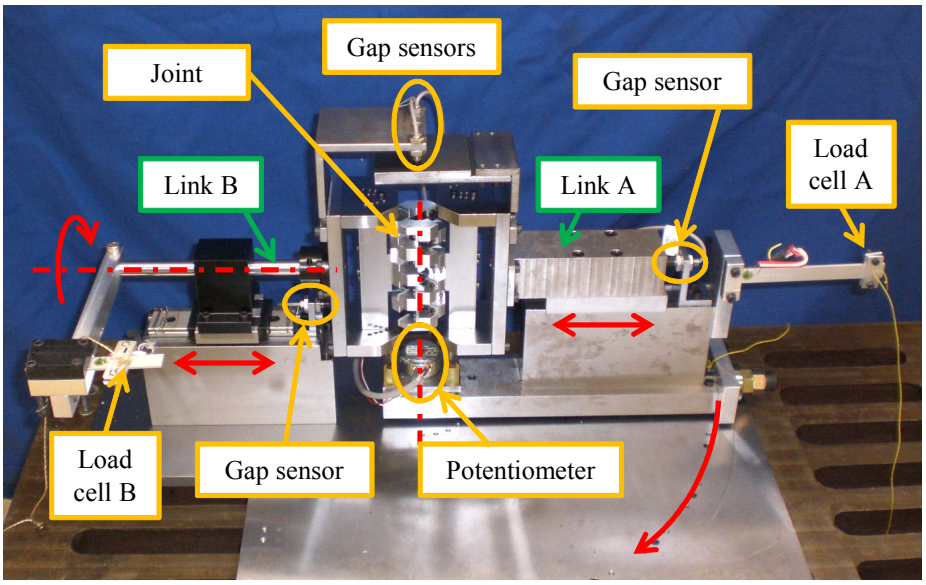

Fig. 7 Overview of experimental apparatus

4. Experimental Analysis of Flexure Revolute Joint

4.1. Experimental Setup

We fabricated experimental flexure revolute joints based on the results in the preceding sections and experimentally investigated their characteristics. A photo of an experimental joint is shown in Fig. 6. The leaf springs are made of hardened steel and the frames are made of duralumin. The mechanical property of the leaf springs is the same as that used in FEA listed in Table 1.

An experimental apparatus to measure the stiffness and axis drift is shown in Fig. 7. The joint was set between the two links A and B. The link A can move around the rotation axis of the joint by an applied force at its tip where a load cell is attached. Since this motion is not a pure rotational motion, coupled motions such as torsional and translational motions with the rotational motion occur as the off-axis motion. The torsional motion of link B and the translational motion of both links relative to the base are not constrained by this apparatus. So, these links can follow the axis drift of the joint when the joint rotates.

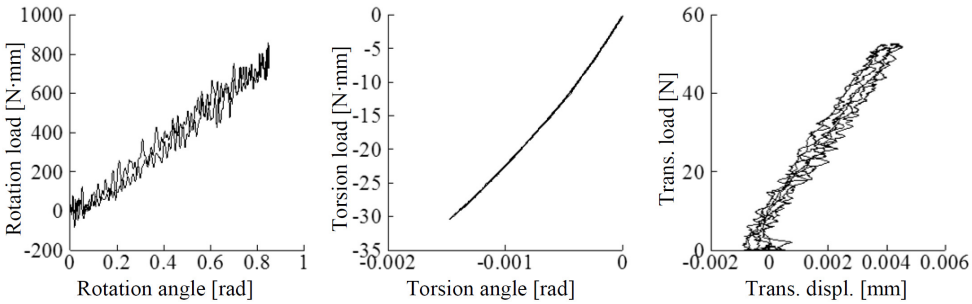

(a) Rotation (b) Torsion (c) Translation

Fig. 8 Displacement-load relationship of the proposed joint obtained by experiments

Table 3 Summary of characteristics of joints

		Proposed joint			CR joint
		Experiment		FEA	
Leaf springs thickness [mm]		0.15	0.1	0.1	(0.8)
Range of motion [deg]		88	≧90	140	34
Stiffness	Rotation [N mm/rad]	9.5×10^{2}	3.1×10^{2}	2.1×10^{2}	9.9×10^{3}
	Torsion [N mm/rad] (Ratio [-])	2.0×10^{6} (2.1×10^{3})	1.5×10^{6} (4.7×10^{3})	1.8×10^{7} (8.5×10^{4})	2.1×10^{6} (2.2×10^{2})
	Translation [N/mm] (Ratio [rad/mm^2])	2.9×10^{3} (3.1)	5.1×10^{3} (16)	3.3×10^{4} (1.6×10^{2})	2.8×10^{3} (0.28)

Rotational and torsional angles and translational displacement were measured with a potentiometer and gap sensors, respectively. Applied loads to generate the rotational, torsional and translational motions were measured by the load cells.

We conducted the following three experiments to investigate the stiffness and axis drift of the joint.

(1) The relationship between rotation angle and rotation moment was measured under the condition where motion of the links was not constrained. The axis drifts with respect to the torsional and translational axes were measured at the same time.

(2) The relationship between the angle and moment of torsion was measured under the condition where the rotation angle was constrained.

(3) The relationship between the translational force applied to the link B and the translational displacement of the link B was measured under the condition where the translational motion of the link A was constrained.

In addition to these three experiments, range of motion of the experimental joint was also investigated.

4.2. Experimental Result

Plastic deformation of leaf springs was observed in the joint with leaf springs of 0.15mm thickness when its rotation angle reached 44 deg in one direction. As for the joint with leaf springs of 0.1mm thickness, any plastic deformation was not observed when the rotation angle was within 45 deg in one direction. Therefore, the experimental joint with leaf springs of 0.1mm thickness can achieve a range of motion of at least 90 deg. This range of motion is remarkably larger than those of conventional flexure revolute joints [2][3].

The displacement-load relationship about each axis is shown in Fig. 8. Small hysteresis are observed in the result with respect to the rotational and translational directions. The main source of these hysteresis is expected to be the friction of the bearings used in the experimental apparatus. The relationships show approximately constant stiffness after the hysteresis effects are withdrawn.

Range of motion and stiffness calculated from the experimental results by the least square approximation are summarized in Table 3. This table includes those values obtained

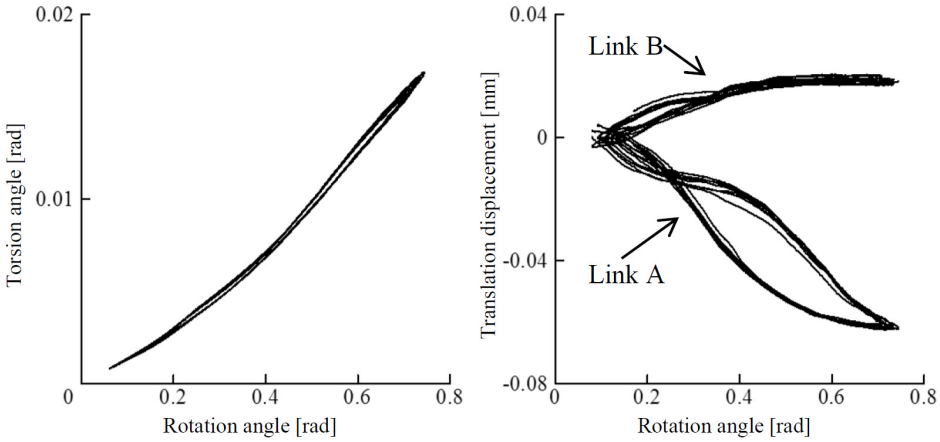

(a) Torsion (b) Translation

Fig. 9 Axis drifts of the proposed joint obtained by experiments

with FEA and those of the CR joint proposed by Trease et al.[2] Although the value obtained by the experiments and FEA with respect to the proposed joint have a similar trend, characteristics obtained by experiments are not as good as those by FEA. The deformation of the frames and fabrication errors, which were not included in FEA, might reduce the off-axis stiffness of the joint. However, the stiffness ratios of the joints are better than those of the conventional joint.

The axis drift with respect to the torsional and translational axes are shown in Fig. 9. The axis drift is not as small as that obtained by FEA. Deformation of the frames and fabrication errors are expected to be some of the sources that caused these axis drifts. However, it is difficult to explain the reason of the complex path of the axis drift shown in the experimental results. We will try to figure out the source of these axis drifts and redesign the joint based on it in our future work.

5. Parallel Robot with the Proposed Joints

5.1. Design and Fabrication

We designed and fabricated a planar five-bar robot with the proposed joints and investigated its characteristics. Robot design was done considering the following three conditions.

(1) The proposed joints are installed at all joints.

(2) Assuming the range of the joints as 45deg, the robot has the workspace of at least 200 mm × 100 mm.

(3) The actuators of the robot are placed on the stationary base.

The overview of the fabricated parallel robot is shown in Fig. 10(a), and link lengths are shown in Fig. 10(b). The link lengths were determined to satisfy the workspace condition considering the motion range of joints.

Detail of the input link, flexure revolute joint on the base and driving arm are shown in Fig. 11. Each input link of the robot is driven by a driving arm attached to a motor. The two motors are placed at isolated positions from the mechanism and set on the stationary base. The driving arm is rigidly connected to the motor but is not rigidly connected to the input link. The input link is held between two cam followers attached to the driving arm. These cam followers don't constrain the translation motion of the input link along its longitudinal direction, which may occur according to the axis-drift of the joint. One of the frames of each joint on the base is directly connected to the base and the other frame is connected to the input link. Frames of the flexure revolute joint are not physically connected to the driving arm. The rotation axis of the driving arm and that of the input link are initially

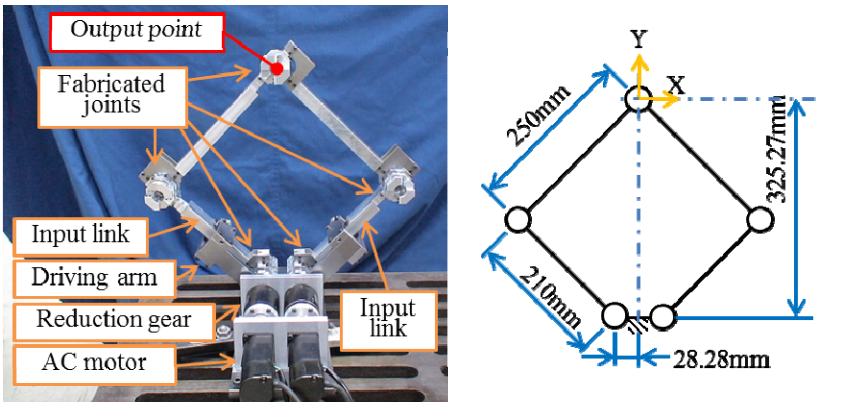

(a) Photo (b) Position of the coordinate frame

Fig. 10 Overview of experimental parallel robot

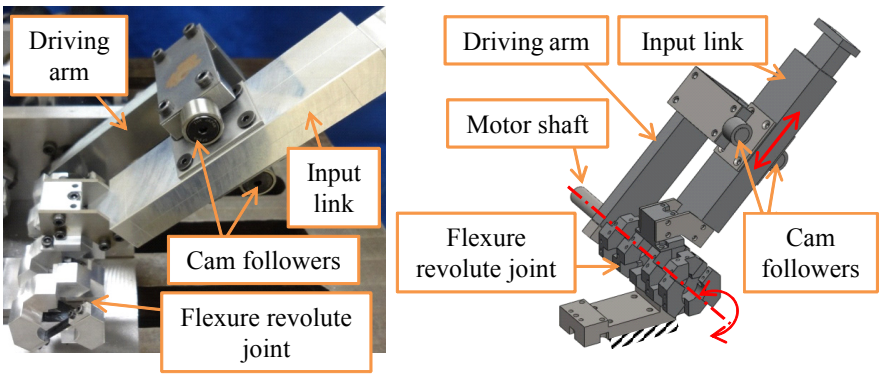

(a) Photo (b) CAD model

Fig. 11 Input link, flexure revolute joint on the base and driving arm

collocated on the same line and their rotation angles would be the same if the drift of the joint is zero.

The robot operates in the vertical plane. The horizontal direction is defined as X axis and the vertical direction is defined as Y axis. Z axis is defined to be perpendicular to the XY plane. The robot was designed and assembled so that all joints are at neutral configurations when the output point of the robot is at the origin of the coordinate frame O. The position of the base coordinate frame relative to the mechanism is shown in Fig. 10(b).

We used a PID controller with torque command while sampling period of control was 1 ms to follow the reference position. Specifications of motors with amplifier were confirmed that they had enough capacity to drive the robot. The PID control system used in experiments is shown in Fig. 12, where $\theta_i, \theta_{\mathrm{ref},i}, \tau_i$ (i: driving arm/motor number) are the actual angle, the reference angle, and the torque command given to the motor driver, and $K_\mathrm{P}, K_\mathrm{I}, K_\mathrm{D}$ are the feedback gains. The PID control system gives the torque command by the following equation.

$$\tau_i = K_\mathrm{P}\left(\theta_{\mathrm{ref},i} - \theta_i\right) + K_\mathrm{I}\int\left(\theta_{\mathrm{ref},i} - \theta\right)dt + K_\mathrm{D}\left(\dot{\theta}_{\mathrm{ref},i} - \dot{\theta}_i\right), \quad (i = 1,2) \tag{1}$$

The reference angle $\theta_{\mathrm{ref},i}$ is calculated by inverse kinematics of planar 5-bar mechanism in which the axis drifts of the flexure joints are neglected.

5.2. Workspace

We gave various positioning and tracking tasks to the robot. The prototype robot achieved these tasks in the workspace of $200\,\mathrm{mm} \times 150\,\mathrm{mm}$. This workspace satisfies the design condition. The volume of this workspace is investigated by the normalized volume

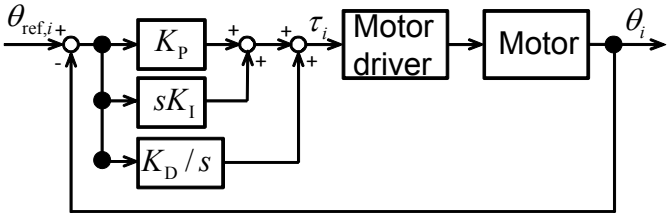

Fig. 12 PID control system

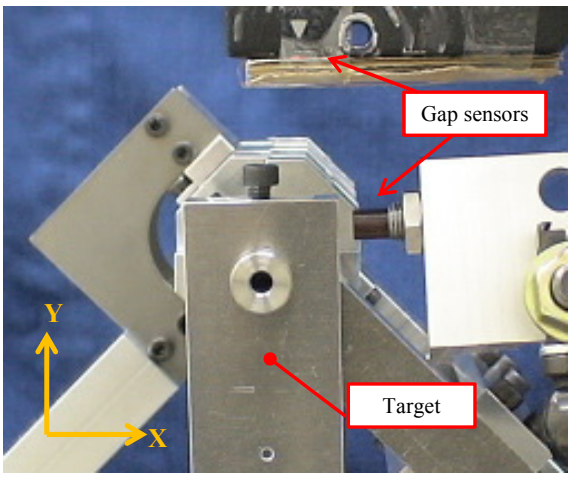

Fig. 13 Sensor target

index (*NVI*). *NVI* proposed by Yang et al.[8] is a non-dimensional index to evaluate a workspace performance of a robot. *NVI* is defined by the following equation for planar robots

$$NVI = \frac{S}{\pi L^2/4}, \tag{2}$$

where S is the area of the actual workspace and L is the maximum reach of the links L. Since the maximum stroke of our robot is about 488mm, its *NVI* is calculated as 0.16. This value of *NVI* is not so large, however, it is compatible to those of conventional robots having closed loops with joints using rigid contacts [8]. Therefore, our robot with the proposed flexure joints can be practically used in many applications.

5.3. Position Repeatability

Position repeatability of the robot was investigated. A sensor target was attached to the output point (Fig. 13) and the horizontal and vertical position deviations of the target during repetitive positioning were measured by two gap sensors. The targets were set on four points: (0, 0), (50, 0), (0, 50), (0, -50) [mm] in O-*XY* plane.

Positioning tests for each target point (X_P, Y_P) were done in which four start positions, (X_P-50, Y_P), (X_P+50, Y_P), (X_P, Y_P-50), (X_P, Y_P+50), were used. The reference trajectory of each driving arm for positioning was generated using the 5-th power polynomial curve as

$$\theta_{\mathrm{ref},i}(t) = \theta_{\mathrm{s},i} + \left(\theta_{\mathrm{t},i} - \theta_{\mathrm{s},i}\right)\left[6\left(\frac{t}{T}\right)^5 - 15\left(\frac{t}{T}\right)^4 + 10\left(\frac{t}{T}\right)^3\right], \quad (i = 1,2) \tag{3}$$

where $\theta_{\mathrm{s},i}$ and $\theta_{\mathrm{t},i}$ are angles of i-th driving arm corresponding to the start and target positions, T is the total time for motion.

Deviations of the realized positions when the same trajectory was used (uni-directional) and when trajectories of different directions were used (multi-directional) were calculated from the measured results. Distributions of measured positions with respect to the averaged

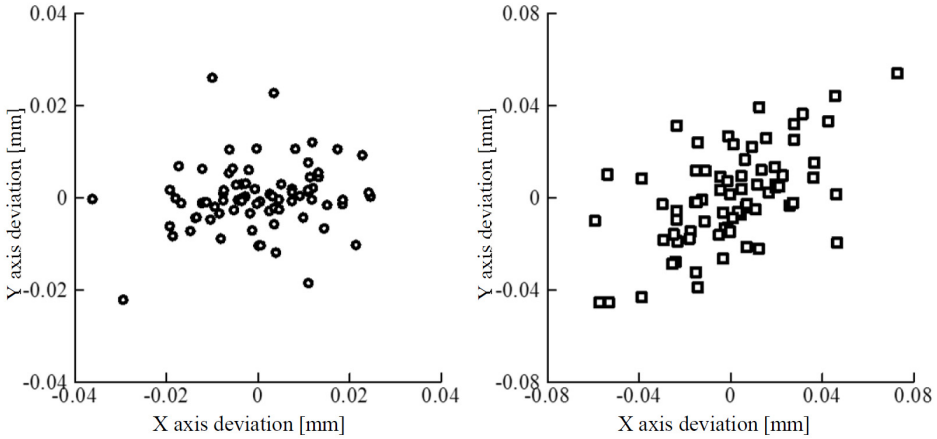

(a) Uni-direction (b)Multi-direction

Fig. 14 Position distributions in positioning by robot

Table 4 Position repeatability of robot

Uni-direction	X axis	0.050mm
	Y axis	0.052mm
Multi-direction	X axis	0.084mm
	Y axis	0.078mm

position are shown in Fig. 14. This figure includes all the data of the measured four target points. Summary of the position repeatability at the measured four points is shown in Table 4. These values were calculated according to ISO9283.

Position repeatability did not reach the expected value considering the mechanical and kinematic properties of the joints and the robot. Dependence of trajectory on the accuracy of the robot can be observed from the fact that the multi-directional repeatability is lower than the uni-directional one. We expect that one of the causes of this problem is the initial compressive deformation of the leaf springs due to the weight of the robot. A snap sound was observed which occurred at the time of the sudden change of the spring shape when the joint of the robot was passing through the neutral configuration in experiments. This sound was not observed when the joint was tested in the experiments in section 4, where external load, which causes initial compressive deformation of leaf springs, was not applied to the joint.

5.4. Stiffness

Stiffness of the robot was also experimentally investigated. A load cell and a gap sensor were used to measure the relationship between the load and the displacement (Fig. 15). This relationship includes the effect of the servo stiffness as well as that by joints and mechanism. In the following discussions, we used the data in which the effect of servo stiffness was removed.

The relationship between the displacement and the load measured at the origin of the coordinate frame is shown in Fig. 15. Although the results show some nonlinearities including hysteresis, the measured relationships have approximately constant stiffness. Stiffness in each direction was calculated by the least square approximation. The calculated stiffness is 33 N/mm in X axis, 16 N/mm in Y axis and 7.5 N/mm in Z axis. These values are smaller than the expected values considering the stiffness of the joints. This is expected to be caused by the initial deformation of the leaf springs mentioned in the previous section.

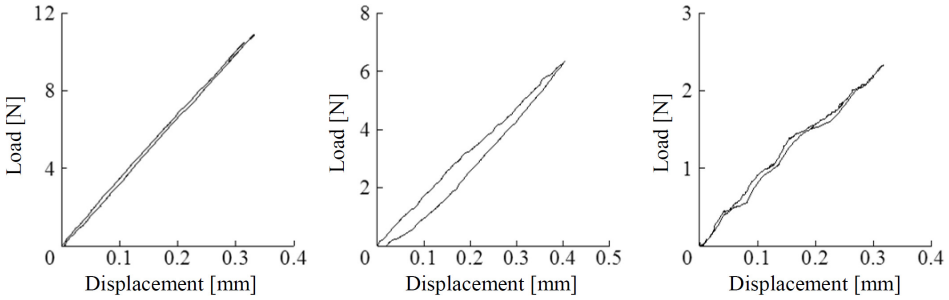

(a) *X* axis (b) *Y* axis (c) *Z* axis

Fig. 15 Displacement-load relationships of the robot

6. Conclusion

This paper proposed a new flexure revolute joint using leaf springs. In the joint, leaf springs connect a pair of frames like a spiral stairs. Arrangement of leaf springs between the two frames was proposed taking into consideration the stiffness characteristics and axis drift of the joint while a large range of motion can be achieved. Characteristics of the joint were investigated by FEA and experiments. The proposed joint actually achieved a large range of motion (at least 90 deg) and a large stiffness ratio comparing to conventional flexure revolute joint. However, a relatively large axis drift was observed in experiments, which was not identified in FEA.

A planar parallel robot with the proposed joints was designed and fabricated. This robot achieved positioning tasks in a large workspace. However, its position repeatability and stiffness did not reach the expected levels considering the characteristics of the joints and the mechanism.

In our future work, we will investigate a more appropriate configuration of the joint to improve the performance, especially in diminishing the axis drift taking into consideration fabrication errors and deformation in frames. We will also investigate the method and mechanism to reduce the effect of initial load on the flexure joints for better performance of parallel robots with the proposed flexure joints.

References

[1] Howell, L., L., “Compliant Mechanisms”, Wiley-intersciense, New York, 2001.

[2] Trease, B., P., Moon, Y.-M., and Kota, S., “Design of Large-Displacement Compliant Joints”, Journal of Mechanical Design, Vol. 127, 2005, pp.788-798.

[3] Zhao, H., and Bi, S., “Accuracy charactoristics of the generalized cross spring pivot”, Mechanism and Machine Theory, Vol. 45, 2010, pp. 1434-1448.

[4] Arata, J., Saito, Y., and Fujimoto, H., “Development of an outer shell type 2 dof bending manipulator using a spring-link mechanism”, Journal of Robotics Society of Japan, Vol. 29, 2011, pp. 523-531(in Japanese).

[5] Pham, H.-H., Chen, I.-M., “Stiffness modeling of flexure parallel mechanism”, Precision Engineering, Vol.29, 2005, pp. 467-478.

[6] Jensen, B., D., Howell, L., L., “The modeling of cross-axis flexural pivots”, Mechanism and Machine Theory, Vol. 37, 2002, pp. 461-476.

[7] Teo, T., J., Chen, I.-M., Yang, G., and Lin, W., “A generic approximation model for analyzing large nonlinear deflection of beam-based flexure joints”, Precision Engineering, Vol. 34, 2010, pp. 607-618.

[8] Yang., D., C., H., and Lin, Y., Y., “Pantograph mechanism as a non-traditional manipulator structure”, Mechanism and Machine Theory, Vol. 20, 1095, pp. 115-122.